Springer

Journal of Mechanical Science and Technology 23 (2009) 2722~2729

Journal of
Mechanical
Science and
Technology

www.springerlink.com/content/1738-494x
DOI 10.1007/s12206-009-0735-3

Numerical experiments on determination of spatially concentrated time-varying loads on a beam: an iterative regularization method †

T. S. Jang* and S. L. Han

Department of Naval Architecture and Ocean Engineering, Pusan National University, Busan 609-735, Korea

(Manuscript Received April 21, 2009; Revised June 26, 2009; Accepted June 29, 2009)

Abstract

This paper treats a solution for the ill-posed (inverse) load determination problem for a time-varying load on a beam. The ill-posed nature of the problem causes numerical instability. Conventional numerical approach for solutions results in arbitrarily large errors in solution. The Tikhonov regularization method, which is a non-iterative stabilization technique, has been widely adopted for overcoming the ill-posed nature (or numerical instability). However, in this paper, we introduce an "iterative" regularization method, specifically, the iterated Tikhonov regularization method. The iterated method is applied to the present load determination problem. The result of the iterative method is compared with that of the (non-iterative) Tikhonov regularization. The rate of convergence for the introduced iterative method turned out to be very fast. The accuracy and applicability of the introduced method are examined through a numerical experiment.

***Keywords*:** Load determination; The iterated Tikhonov regularization; Iterative and non-iterative regularization; Ill-posed problem

1. Introduction

For design and health monitoring of mechanical dynamic structures, one has to determine the real and exact time-varying external loads which act on the structural systems. However, not only extremely large magnitudes of loads, such as impact loads, but problems in the installation of load-measurement devices make it, in practice, sometimes difficult to directly measure the external dynamic loads. Accordingly, inverse procedures are needed for indirectly measuring the time-varying loads.

In general, in contrast to finding the displacement of a structural system subjected to given time-varying external loads, the (inverse) problem of determining external loads from the measured displacement is difficult in calculating accurate results. This would be mainly caused by the ill-posed nature (or instability) arising from the inverse determination problem: the solution lacks stability property. Thus, the solution of external load does not depend on the given measured data of dynamic response in a stable (or continuous) manner. In consequence, a small amount of noisy data in a measured dynamic response can be extremely amplified and may lead to unreliable solutions of time-varying loads. For overcoming this difficulty of instability, it is essential to employ a stabilization technique for stable solutions.

There have been many research works on the modification of stabilization technique and the related inverse load determination problem. Inoue et al. [1] treat an inverse problem to estimate the magnitude and direction of impact load acting on a body of arbitrary shape based on the singular value decomposition. Wang et al. [2] present a predictive model based on the Tikhonov regularization method for determining the location and amplitude of an unknown impact load acting on a simply supported beam. Hashemi and

† This paper was recommended for publication in revised form by Associate Editor Jeonghoon Yoo
*Corresponding author. Tel.: +82 51 510 2789, Fax.: +82 51 581 3718
E-mail address: taek@pusan.ac.kr
© KSME & Springer 2009

Kargarnovin [3] present the identification method for the amplitude of the impact load acting on a simply supported beam and its location using the genetic algorithm. Gunawan et al. [4] proposed two-step b-spline regularization method for solving an ill-posed problem of impact-load reconstruction. Gunawan et al. [5] also proposed a method to approximate the impact-load by quadratic spline approximation. For some load inverse problems, a method based on the least-square is adopted to recover the load acting on ceramic body armor [6].

For the stable solutions, most of the research works depend on Tikhonov regularization method, characterized as a non-iterative stabilization technique. However, in the present study, an iterative stabilization technique is introduced and applied for obtaining the time-varying load on a simply supported beam. Specifically, we use the iterated Tikhonov regularization method to yield numerical iterative solutions. The numerical result of the iterated Tikhonov regularization is compared with that of the non-iterated Tikhonov regularization. A comparison study illustrates that the introduced iterated Tikhonov regularization is applicable to the inverse load determination problem. In addition, it provides more accurate numerical solutions of time-varying loads acting on the beam than those of the non-iterative case of the Tikhonov method.

2. Review of the beam equation

We consider a simply supported beam subject to an external load $F(x,t)$, as shown in Fig.1. The beam is assumed to be of constant mass ρ per unit length having linear viscous damping C, constant flexural stiffness EI, and a span length L. Neglecting the effect of the shear deformation and rotary inertia, we have the equation of motion for Euler-Bernoulli beam, expressed as [7]

$$\rho\frac{\partial^2 v(x,t)}{\partial t^2}+C\frac{\partial v(x,t)}{\partial t}+EI\frac{\partial^4 v(x,t)}{\partial x^4}=F(x,t) \quad (1)$$

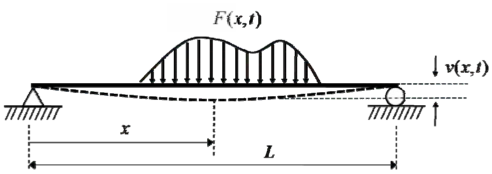

Fig. 1. Definition sketch for a simply supported beam under the circumstance of external load.

with the boundary conditions at $x=0$ and L:

$$v(0,t)=0, \quad \frac{\partial^2 v(0,t)}{\partial x^2}=0\text{, and} \quad (2)$$

$$v(L,t)=0, \quad \frac{\partial^2 v(L,t)}{\partial x^2}=0 \quad (3)$$

In Eq. (1), $v(x,t)$ stands for the vertical displacement of the beam at a distance x and time t and $F(x,t)$ for an external load acting on the beam.

Suppose that a spatially concentrated time-varying load is applied at $x=a$ as depicted in Fig. 2. Eq. (1) then becomes

$$\rho\frac{\partial^2 v(x,t)}{\partial t^2}+C\frac{\partial v(x,t)}{\partial t}+EI\frac{\partial^4 v(x,t)}{\partial x^4}=f(t)\delta(x-a) \quad (4)$$

where δ denotes the delta function. Based on the expansion theorem for orthogonal functions, we can expand the dynamic displacement $v(x,t)$ as

$$v(x,t)=\sum_{n=1}^{\infty}\phi_n(x)q_n(t) \quad (5)$$

where $\phi_n(x)$ and $q_n(t)$ represent mode shape functions (or orthogonal eigenfunctions) and modal displacements, respectively, with the mode number n. After substituting the eigenfunction expansion (5) into Eq. (4), and the multiplication of $\phi_l(x)$ and integration with respect to x over the beam length, we obtain an infinite set of equations of motion for the modal displacement $q_n(t)$:

$$\frac{d^2q_n(t)}{dt^2}+2\xi_n\omega_n\frac{dq_n(t)}{dt}+\omega_n{}^2q_n(t)=F_n(t), \quad n=1,2,... \quad (6)$$

In Eq. (6), ω_n, ξ_n, $F_n(t)$ denote modal frequency, the damping ratio and the modal load for the nth mode, respectively. The modal parameters can be

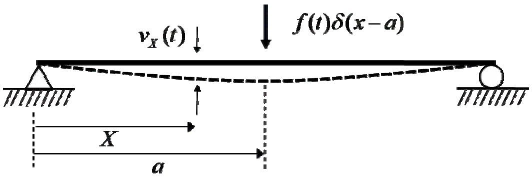

Fig. 2. Spatially concentrated time-varying load acting on a simply supported beam.

expressed as follows:

$$\omega_n = (n^2\pi^2 / L^2)\sqrt{\frac{EI}{\rho}} \tag{7}$$

$$\xi_n = \frac{C}{2\rho\omega_n} \tag{8}$$

$$\phi_n(x) = \sin\left(\frac{n\pi x}{L}\right) \tag{9}$$

$$F_n(t) = f(t)\phi_n(a) \tag{10}$$

The solution of Eq. (6) can be derived as the convolution integral:

$$q_n(t) = \frac{1}{\omega_n'}\int_0^t f(\tau)\ \phi_n(a)e^{-\xi_n\omega_n(t-\tau)} \sin\omega_n'(t-\tau)d\tau, \quad n=1,2,... \tag{11}$$

with the zero initial conditions: $v(x,0) = \partial v/\partial x(x,0) = 0$. In Eq. (11), $\omega_n' = \omega_n\sqrt{1-\xi_n^{\ 2}}$. Substitution of Eq. (11) into Eq. (5) gives the dynamic displacement $v\ (x,t)$ for the beam, subject to a spatially concentrated time-varying load acting at $x = a$:

$$v(x,t) = \int_0^t \sum_{n=1}^{\infty} \frac{\phi_n(x)\phi_n(a)}{\omega_n'} f(\tau)e^{-\xi_n\omega_n(t-\tau)} \sin\omega_n'(t-\tau)d\tau \tag{12}$$

3. Inverse formulation

The need to formulate a functional relation between the time-varying dynamic load and the corresponding dynamic response of the beam arises in connection with the inverse load determination. Suppose that we measure a dynamic displacement of the beam at a fixed position $x = X$: this shall be denoted by $v_X(t) = v(X,t)$. The time-varying load can then be determined by solving following integral equation:

$$v_X(t) = \int_0^t K(t,\tau;X)f(\tau)d\tau \tag{13}$$

where the kernel K of the integral Eq. (13) is defined as

$$K(t,\tau;X) = \sum_{n=1}^{\infty} \frac{\phi_n(X)\phi_n(a)}{\omega_n'} e^{-\xi_n\omega_n(t-\tau)} \sin\omega_n'(t-\tau) \tag{14}$$

Eq. (13) may be represented in abbreviated or symbolic form, as

$$v_X(t) = \mathfrak{L}(f) \tag{15}$$

where the operator $\mathfrak{L}$ is defined as

$$\mathfrak{L}(f) = \int_0^t K(t,\tau;X)f(\tau)d\tau \tag{16}$$

The inverse problem formulated in Eq. (13) is a Volterra-type of integral equation of the first kind, for the time-varying load $f(t)$. According to theory of integral equations [8], the "first" kind integral equation with the regular kernel such as K in Eq. (14) is "ill-posed" in the sense of stability. This leads to numerical instability in solution, that is, the solution lacks stability property, which will strongly affect the performance of the inverse load determination.

4. Calculation of spatially concentrated time-varying load

4.1 Non-Iterative stabilization: Tikhonov Regularization

Since the load determination problem formulated herein is ill-posed, as mentioned in the previous section, conventional numerical methods do not give stable solutions. For stable solutions, we first introduce Tikhonov's regularization method as a stabilization technique.

Tikhonov [9] introduced a functional M which has a damping term Ω with a positive real number λ, called the regularization parameter, to regularize (or stabilize) the Volterra, integral equation of Eq. (13): for a positive real number T,

$$M = \left\{\int_0^T \left|\int_0^t K(t,\tau;X)f(\tau)d\tau - v_X(t)\right|^2 dt\right\}^{1/2} + \lambda\,\Omega, \tag{17}$$

In Eq. (17), $v_X(t)$ is assumed to be a known quantity, or a measured displacement of the beam on a finite time-interval:

$$\Gamma = (0,T)\ . \tag{18}$$

The functional M in Eq. (17) is the Tikhonov functional in which the additional term Ω is defined as follows:

$$\Omega = \int_0^T |f(t)|^2\ dt \tag{19}$$

It is known that Tikhonov functional M has a unique minimum $f(t)$ and this minimum satisfies the integral equation of the second kind [9]:

$$\lambda f + \mathfrak{L}^*\mathfrak{L}(f) = \mathfrak{L}^*(v_X) \,, \quad (20)$$

where $\mathfrak{L}^*$ is the adjoint operator: for some function g,

$$\mathfrak{L}^* g = \int_0^t \overline{K(\tau,t;X)} g(t) dt \,. \quad (21)$$

Eq. (20) can be solved to yield a stable solution of the time-varying load $f(t)$ because the "second" kind integral Eq. (20) is known as a well-posed problem in the solution stability.

4.2 Optimal choice of the regularization parameter: L-curve criterion

According to the regularization theory, regularization parameter λ for the Tikhonov regularization plays an important role in applying the regularization process. In this paper, the L-curve criterion is introduced for choosing an optimal regularization parameter. The L-curve is represented as a log-log plot $(\log\|\mathfrak{L}f - v_x\|, \log\|f\|)$ of the norm of the residual versus the corresponding norm of a regularized solution. The log-log plot generally gives a typical "L" shape, and the optimal value for the regularization parameter is considered to be the one that corresponds to the corner of the curve [10, 11].

4.3 Iterative stabilization: the iterated Tikhonov regularization

In contrast to the non-iterative case discussed above, in this subsection, we introduce the iterated Tikhonov regularization, expressed as follows [8]: for a positive convergence parameter β,

$$\left\{\beta I + \mathfrak{L}^*\mathfrak{L}\right\}(f_{m+1}) = \mathfrak{L}^*(v_X) + \beta f_m, \qquad m = 0,1,2,... \quad (22)$$

In the process of iteration in Eq. (22), the initial guess for the desired load is assumed to be the zero function: $f_0=0$. In Eq. (22), the number of iterations m is called the discrete regularization parameter. In Eq. (22), the convergence parameter β can be chosen, so that the size of the residual $\|\mathfrak{L}f - v_x\|$ is the same as the error level in the data: $\|\mathfrak{L}f - v_{X,Noisy}\| = \delta$ where δ is defined as $\|v_X - v_{X,Noisy}\| \le \delta$. This process is known as Morozov's discrepancy principle [8, 12].

5. Numerical Experiments

In this section, we will examine a numerical example of the inverse determination of the spatially concentrated time-varying load f. For this purpose, we consider the following form of time-varying load, applied to the simply supported beam., as shown in Figs. 1 and 2, at $x=0.25m$: for convenience, σ is chosen as 10^{-2},

$$f(t) = \frac{10t}{\sigma^2} e^{(-t^2/2\sigma^2)} \,. \quad (23)$$

The corresponding dynamic response becomes

$$v_X(t) = \int_0^t K(t,\tau;X) f(\tau) d\tau$$
$$\approx \int_0^t \sum_{n=1}^{M} \frac{\phi_n(X)\phi_n(a)}{\omega_n'} \frac{10\tau}{\sigma^2} e^{(-\tau^2/2\sigma^2)} e^{-\xi_n\omega_n(t-\tau)} \sin\omega_n'(t-\tau) d\tau \quad (24)$$

For the present numerical simulation, we choose $M=10$ in Eq. (24). The physical properties for the beam are given as $EI=23KNm^2$, $L=1m$, $\rho=48.2kg/m$, and $C=15\rho$. A simple numerical integration in Eq. (23) gives the time history of the displacement of the beam, which is illustrated in Fig. 3(a): we choose $T=0.2s$.

Now, our aim is to inversely determine the time-varying load f in Eq. (23) by using measured data of the beam displacement in Eq. (24). However, in practice, the measured data for the displacement of the beam is always deteriorated by noise to an extent [11].

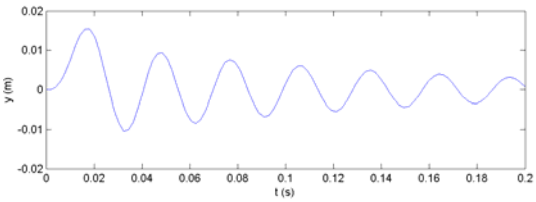

(a) Noise-free displacement

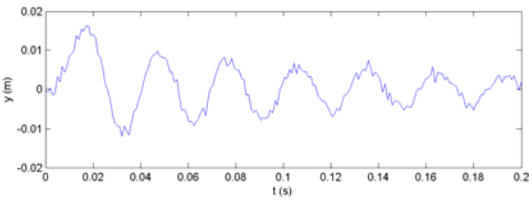

(b) Noisy data with error level 3.2%,

Fig. 3. Time history of vertical displacement of the beam in Eq. (24).

Let us denote the (noisy) measured data by $v_{X,Noisy}$. In the present numerical experiments, we randomly generate the measurement noises from electrical and thermal fluctuation and quantization error. The additive noise is assumed to have the normal distribution with zero mean. The error level for the measured data is usually defined as

$$\left\| \frac{v_{X,Noisy} - v_X}{v_X} \right\|_2 \times 100\% \quad \text{where } \| \cdot \|_2 \equiv \sqrt{\int_0^T | \cdot |^2 \, dt} \tag{25}$$

In the study, the error level is chosen to be *3.2%* and the time history of the noisy data is illustrated in Fig. 3(b).

5.1 A Conventional numerical approach

Now, we attempt to recover the time-varying load in Eq. (23) by using the dynamic response data in Fig. 3(b). For the purpose, we directly discretize (13) with a conventional quadrature integration rule: we approximate Eq. (13) by

$$v_X(t_i) = h\sum_{j=0}^{i} w_{ij}\, K(t_i, \tau_j) f(\tau_j), \quad i = 0, 1, \cdots, N \tag{26}$$

where w_{ij} denotes quadrature weights and h is the sampling time $h=T/N$. h in Eq. (26) is chosen to be *0.001s.*

It is convenient to rewrite Eq. (26) in the matrix-vector form as

$$\mathbf{v} = \mathbf{L}\mathbf{f} \tag{27}$$

In Eq. (27), the symbols $\mathbf{v}$ and $\mathbf{f}$ represent column vectors of the beam displacement and the (unknown) time-varying load, respectively. The symbol $\mathbf{L}$ is a matrix relation from $\mathbf{f}$ to $\mathbf{v}$, which corresponds to the operator $\mathfrak{L}$ in Eq. (16). The solution for Eq. (27) is illustrated in Fig. 4. As expected, we have an unstable solution. This instability in the numerical solution mainly results from the inherent nature of the ill-posed problem in the sense of stability. Thus, we move to the next subsection to investigate a stabilization technique for obtaining stable solutions.

5.2 Stabilization techniques

In a similar manner to Eq. (26), Tikhonov's regularization method in Eq. (20), is readily discretized as

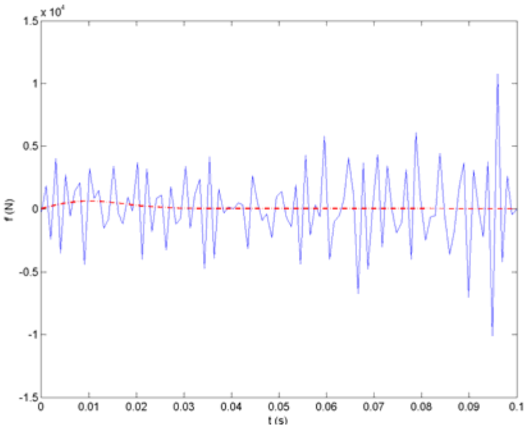

Fig. 4. Typical solution by a conventional numerical scheme (solid lines) and the exact solution (red-dashed).

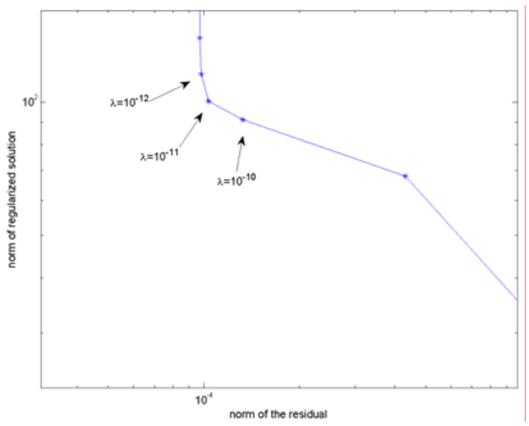

(a) L-curve for the Tikhonov regularization

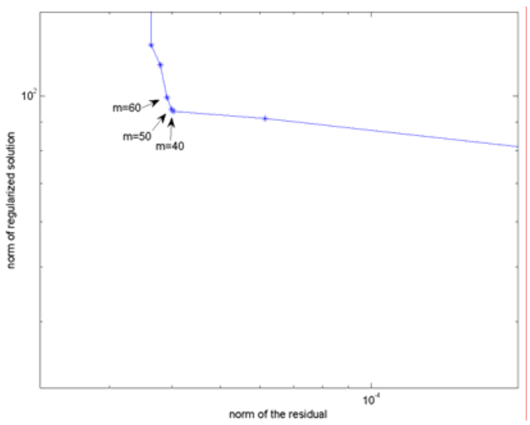

(b) L-curve for the iterated Tikhonov regularization

Fig. 5. L-curve criterion.

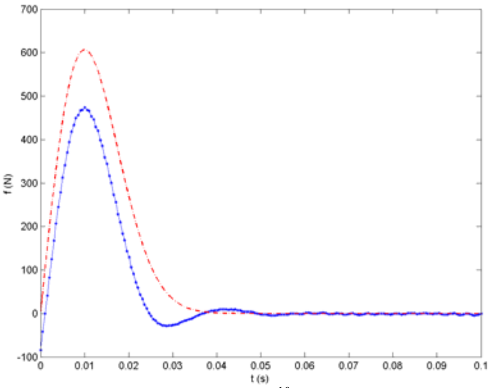

(a) λ=10^{-10}

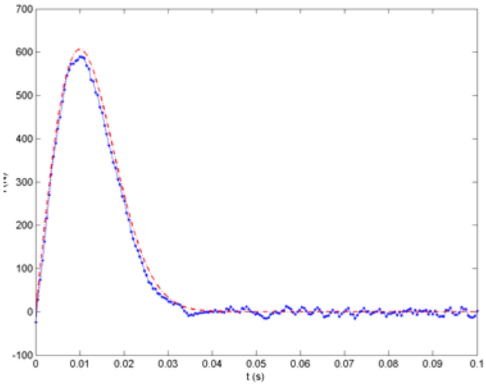

(b) λ=10^{-11}

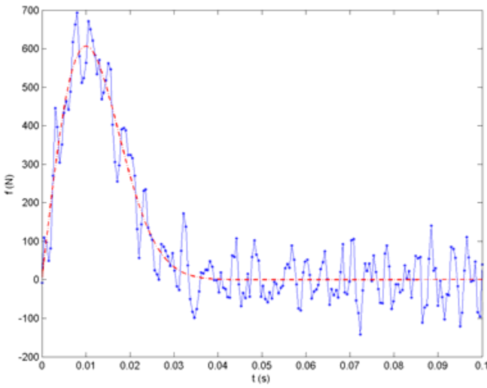

(c) λ=10^{-13}

Fig. 6. Regularized solutions with Tikhonov regularization.
Legend: The red-dashed and blue-dotted lines respectively stand for the exact solution f in Eq. (23) and the numerical solution with the Tikhonov regularization in Eq. (28).

$$\lambda \mathbf{f} + \mathbf{L}^H \mathbf{L} \mathbf{f} = \mathbf{L}^H \mathbf{v} \tag{28}$$

where H indicates Hermitian transpose. The numerical solution for the linear system (28) is depicted in

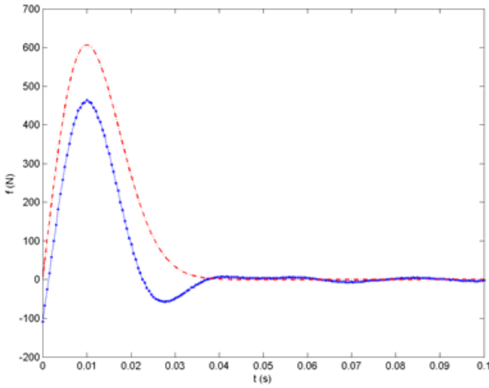

(a) m=5

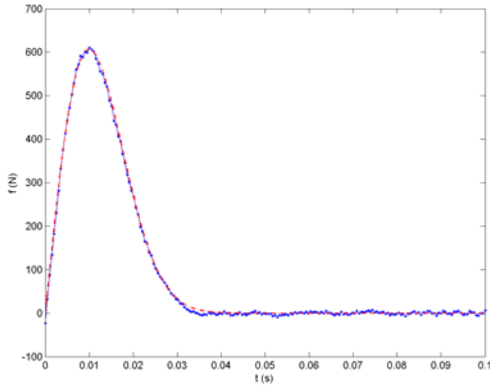

(b) m=50

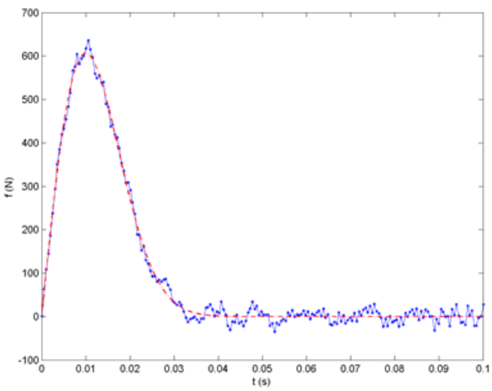

(c) m=100

Fig. 7. Regularized solutions with the iterated Tikhonov regularization with β=10^{-9}.
Legend: The red-dashed and blue-dotted lines respectively stand for the exact solution f in Eq. (23) and the numerical solution with the iterated Tikhonov regularization in Eq. (29).

Fig. 6 in which the noisy data of the beam displacement in Fig. 3(b) is used for $\mathbf{v}$ in Eq. (28): three different regularization parameters are presented for the Tikhonov solutions. The most accurate solution can be found when the regularization parameter $\lambda = 10^{-11}$. This is confirmed by the result of the L-curve criterion as shown in Fig. 5: the point $\lambda = 10^{-11}$ in Fig. 5(a) is the one corresponding to the corner of the curve, as explained in section 4.2.

The discretized form which corresponds to the iterated Tikhonov's regularization method in Eq. (22) is written as

$$\left\{ \beta \mathbf{I} + \mathbf{L}^H \mathbf{L} \right\} (\mathbf{f}_{m+1}) = \mathbf{L}^H (\mathbf{v}) + \beta \mathbf{f}_m, \quad m = 0,1,2,... \quad (29)$$

Fig. 7 pictures the numerical results for Eq. (29) for three different numbers of iterations m: a positive convergence parameter β can be chosen to satisfy Morozov's discrepancy principle [8, 12] as discussed in section 4.3, and in this paper the parameter is chosen as 10^{-9}. Among them, we find the most accurate solution when m=50. This is justified by the fact that m=50 corresponds to the corner of the curve in Fig. 5(b): see section 4.2.

Finally, we compare the accuracy of the two regularization methods. The error for numerical solutions is usually defined as follows:

$$err = \frac{\left\| f_{Exact}(t) - f_{Reg}(t) \right\|_2}{\left\| f_{Exact}(t) \right\|_2} \times 100 \quad \text{where } \| \cdot \|_2 \equiv \sqrt{\int_0^T \left| \cdot \right|^2 dt} \quad (30)$$

where $f_{Exact}(t)$ and $f_{\mathrm{Reg}}(t)$ denote the exact solution in Eq. (23) and the numerical solution obtained by using the regularization methods, respectively. From the calculation, the errors are found to be 12.42% and 6.686% for the Tikhonov regularization method and the iterated Tikhonov regularization method, respectively. Thus, at least, in the present numerical experiments, it is concluded that more accurate numerical solutions can be obtained by using the iterated Tikhonov regularization method rather than the Tikhonov regularization method.

6. Conclusion

We have introduced an iterative regularization method (the iterated Tikhonov regularization) to determine the external time-varying load on a simply supported beam. By using the measured vertical displacement of the beam, the time history of external load is determined. The numerical experiments demonstrated that the iterated Tikhonov regularization method is able to yield a quite accurate solution, even though the measured response data is contaminated by noise. In addition, the convergence rate for the solution is very fast. At least in the case of the presented numerical experiment, we obtain a more accurate solution from the iterated Tikhonov regularization than that from the Tikhonov regularization method.

Acknowledgment

This work was supported for two years by Pusan National University Research Grant.

References

[1] B. T. Wang and C. H. Chiu, Determination of unknown impact force acting on a simply supported beam, *Mechanical System and Signal Processing* **17** (2003) 683-704.

[2] H. Inoue, N. Ikeda, K. Kishimoto, T. Shibuya and T. Koizumi, Inverse analysis of the magnitude and direction of impact force, *JSME International Journal Series A* **38** (1995) 84− 91.

[3] R. Hashemi and M. H. Kargarnovin, Vibration base identification of impact force using genetic algorithm, *International Journal of Mechanical Systems Science and Engineering* **1** (2007) 204-210.

[4] F. E. Gunawan, H. Homma and Y. Kanto, Two-step B-splines regularization method for solving an ill-posed problem of impact-force reconstruction, *Journal of Sound and Vibration* **297** (2006) 200-214.

[5] F. E. Gunawan, H. Homma and Y. Morisawa, Impact-Force estimation by quadratic spline approximation, *Journal of Solid Mechanics and Materials Engineering* **2** (2008) 1092-1103.

[6] A. A. Cardi, D. E. Adams and S. Walsh, Ceramic body armor single impact force identification on a compliant torso using acceleration response mapping, *Structural health monitoring* **5** (2006) 355-372.

[7] L. Meirovitch, *Analytical Methods in Vibrations*. London, UK: The MacMillan Company (1967).

[8] A. Kirsch, *An Introduction to the Mathematical Theory of Inverse Problems*. Springer (1996).

[9] A. N. Tikhonov, Solution of incorrectly formulated

problems and the regularization method. *Sov. Doklady* **4** (1963) 1035-1038.

[10] P. C. Hansen, Analysis of discrete ill-posed problems by means of the L-curve, *SIAM Review* **34** (1992) 561-580.

[11] T. S. Jang, H. G. Sung, S. L. Han and S. H. Kwon, Inverse determination of the loading source of the infinite beam on elastic foundation, *Journal of Mechanical Science and Technology* **22** (2008) 2350-2356.

[12] T. S. Jang, H. S. Choi and T. Kinoshita, Numerical experiments on an ill-posed inverse problem for a given velocity around a hydrofoil by iterative and noniterative regularizations, *Journal of Marine Science and Technology* **5** (2000) 107-111.

Taek Soo Jang, the corresponding author of the paper, is by birth a Korean, with Naval Architecture and Ocean Engineering Ph.D degree from Seoul National University, who worked at the department of Naval Architecture and Ocean Engineering in Pusan National University from 2003 until now. His main field of research has been the optimization theory, water wave motion and inverse problem with special focus on ocean-related fields